RadioGraphics

An Investigation of Operator Exposure in Interventional Radiology[1]

Beth A. Schueler, PhD • Thomas J. Vrieze, RT(R) • Haraldur Bjarnason, MD • Anthony W. Stanson, MD

TEACHING POINTS
See last page

A study was conducted to investigate how operator exposure in interventional radiology is affected by various common fluoroscopic imaging conditions. Stray radiation levels surrounding the imaging chain of a C-arm angiographic system were measured with an anthropomorphic abdomen phantom under different imaging conditions, and isodose curves were constructed. Operator exposure was shown to increase with patient dose-area product as the imaging field of view (FOV) is changed, with the highest scatter levels occurring with an intermediate-sized FOV. Use of copper spectral beam filtration was found to result in decreased operator exposure, whereas use of wedge-shaped equalization filters was found to increase exposure. The effect of increasing patient abdomen thickness was simulated by surrounding the phantom with plastic bolus material. Increasing the thickness by 5 cm resulted in a doubling of exposure at the operator's waist. Exposure to the operator's upper body was significantly reduced when the FOV was positioned on the far side of the patient. Operator exposure can be maintained at an acceptable level by taking these variables into consideration and incorporating the suggested dose reduction techniques into routine practice to the greatest extent possible.

Abbreviations: DAP = dose-area product, FOV = field of view, II = image intensifier

RadioGraphics 2006; 26:1533–1541 • **Published online** 10.1148/rg.265055127 • **Content Codes:** PH QA VI

[1]From the Department of Radiology, Mayo Clinic, 200 First St SW, Rochester, MN 55905. Recipient of a Certificate of Merit award for an education exhibit at the 2002 RSNA Annual Meeting. Received June 7, 2005; revision requested July 26 and received October 10; accepted October 10. All authors have no financial relationships to disclose. **Address correspondence to** B.A.S. (e-mail: *schueler.beth@mayo.edu*).

See the commentary by Coldwell following this article.

Introduction

It has been shown that radiologists who perform interventional procedures may potentially receive high radiation doses (1–5). The common radiation protection principles with regard to time, distance, and shielding are difficult for operators to fully implement in interventional procedures due to examination complexity, the required proximity of the operator to the patient, and the need to maintain a sterile field. Increases in interventional procedure difficulty, volumes, and workload per radiologist also contribute to the high radiation levels. To help operators minimize dose, training in radiation protection and education about stray radiation sources are essential (6–8).

In this study, we measured the magnitude and distribution of stray radiation at the radiologist's position under various fluoroscopic imaging conditions. These conditions included use of selectable angiography equipment features (field size, beam filtration, equalization filters), along with noncontrollable clinical situations (patient abdomen thickness and position). The imaging equipment and operator's position investigated in this article are specific to abdominal interventional radiology procedures performed on a C-arm angiographic system. However, certain aspects of the results are relevant to all fluoroscopic procedures.

Materials and Methods

Various clinical imaging conditions that are typical in interventional procedures were simulated using a patient-equivalent abdomen phantom (The Phantom Laboratory, Salem, NY), which included a human skeleton with simulated organs surrounded by soft tissue–equivalent material. The phantom was imaged with a C-arm angiographic system (Polytron; Siemens Medical Solutions, Erlangen, Germany) equipped with a 40-cm image intensifier (II). All stray radiation levels were measured during continuous fluoroscopy under automatic exposure control. The II input exposure rate was set at 0.32 μGy/sec with a 28-cm imaging field of view (FOV). With no added copper spectral beam filtration, the half value layer was 3.4 mm aluminum at 80 kVp. To mimic a typical clinical geometric configuration,

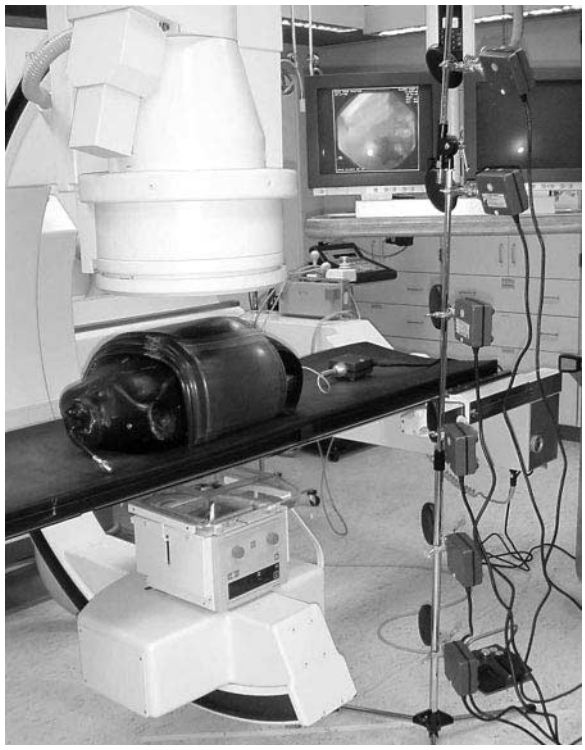

Figure 1. Photograph shows the angiographic C arm and the abdomen phantom with an additional 5-cm of bolus material and six ionization chambers positioned to acquire stray radiation measurements on a 30-cm grid.

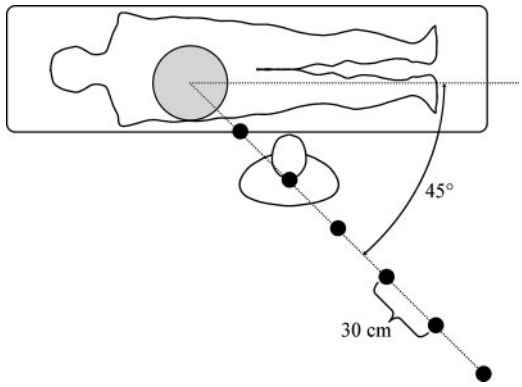

Figure 2. Drawing illustrates the location of the FOV (gray circle), the operator's expected position for right femoral access, and the location of measurement positions (●) at 30-cm intervals along a vertical plane angled 45° from the table.

the distance from the floor to the phantom entrance surface was set at 90 cm. The x-ray source was positioned under the table at a distance of 52 cm from the phantom entrance surface. The II

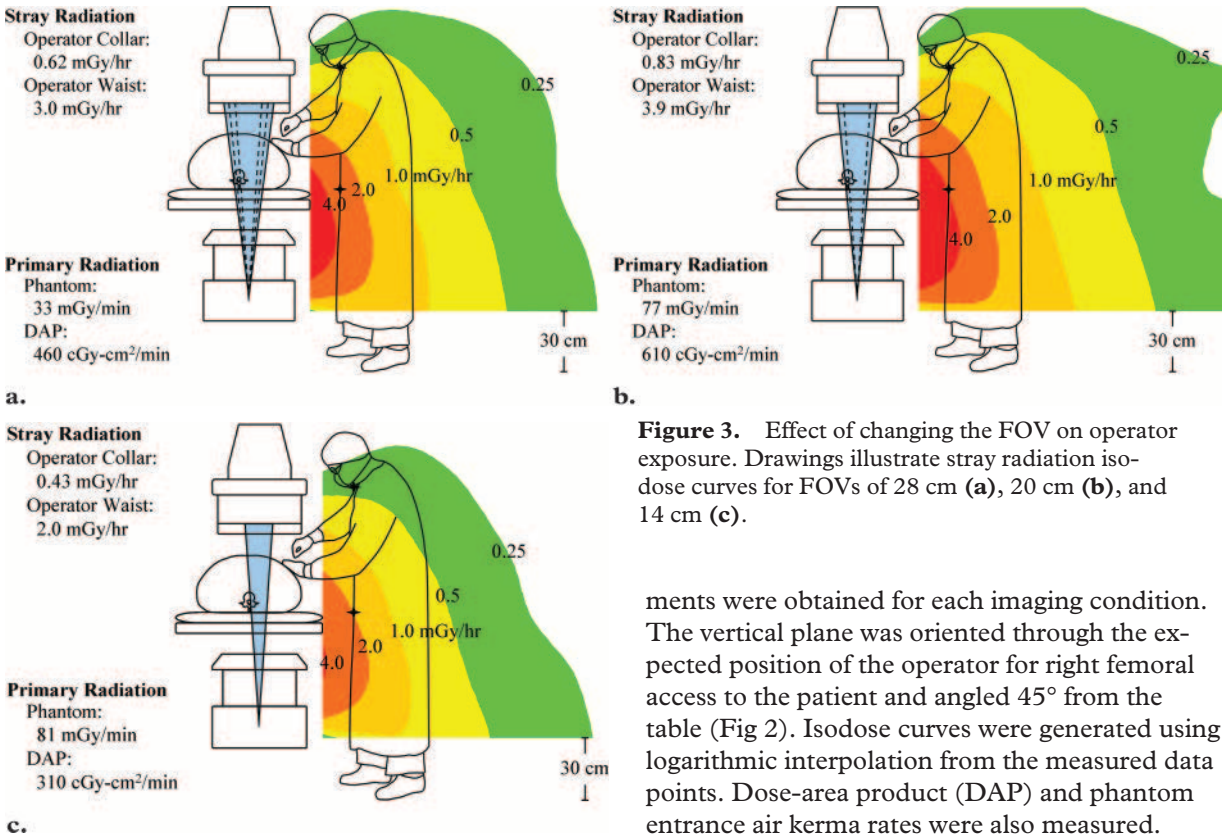

Figure 3. Effect of changing the FOV on operator exposure. Drawings illustrate stray radiation isodose curves for FOVs of 28 cm **(a)**, 20 cm **(b)**, and 14 cm **(c)**.

height was adjusted to maintain a distance of 10 cm between the phantom exit surface and the entrance to the II assembly. To simulate larger patient sizes, plastic bolus material (Bolx-II; MedTec, Orange City, Iowa) was placed around the phantom (Fig 1). Unless otherwise noted, a standard imaging protocol was used for all measurements: an abdomen phantom with 5 cm of added bolus material and a 28-cm FOV, with the radiation field centered over the liver region. For the standard imaging protocol, the automatic exposure control maintained the tube voltage at 80 kVp. Variables included FOV size, amount of copper spectral beam filtration, patient abdomen thickness, patient position, and use of an equalization filter.

Stray radiation air kerma rates were recorded with six ionization chambers (10X5–180, Model 1015; Radcal, Monrovia, Calif) positioned 30, 60, 90, 120, 150, and 180 cm above the floor. Measurements were acquired in a vertical plane by positioning the six chambers at a distance of 30, 60, 90, 120, 150, and 180 cm from the x-ray beam central ray, with the result that 36 measurements were obtained for each imaging condition. The vertical plane was oriented through the expected position of the operator for right femoral access to the patient and angled 45° from the table (Fig 2). Isodose curves were generated using logarithmic interpolation from the measured data points. Dose-area product (DAP) and phantom entrance air kerma rates were also measured. Stray radiation air kerma rates were estimated for the expected position of the operator's collar and waist 45 cm from the x-ray beam central ray and 150 and 90 cm from the floor, respectively.

Results

Effect of Changing the FOV

The stray radiation distribution was compared for FOVs of 28, 20, and 14 cm. For each measurement, the central ray remained at the same location, centered over the area of the liver (Fig 3). When the FOV was reduced from 28 to 20 cm, the phantom entrance air kerma rate more than doubled and the stray radiation dose rates increased by approximately 30% at both the operator's waist and collar. When the FOV was further reduced from 20 to 14 cm, the phantom entrance air kerma rate increased only slightly and the stray radiation dose rates dropped by approximately 50% at the operator's waist and collar. Thus, operator exposure was highest with the intermediate-sized FOV (20 cm).

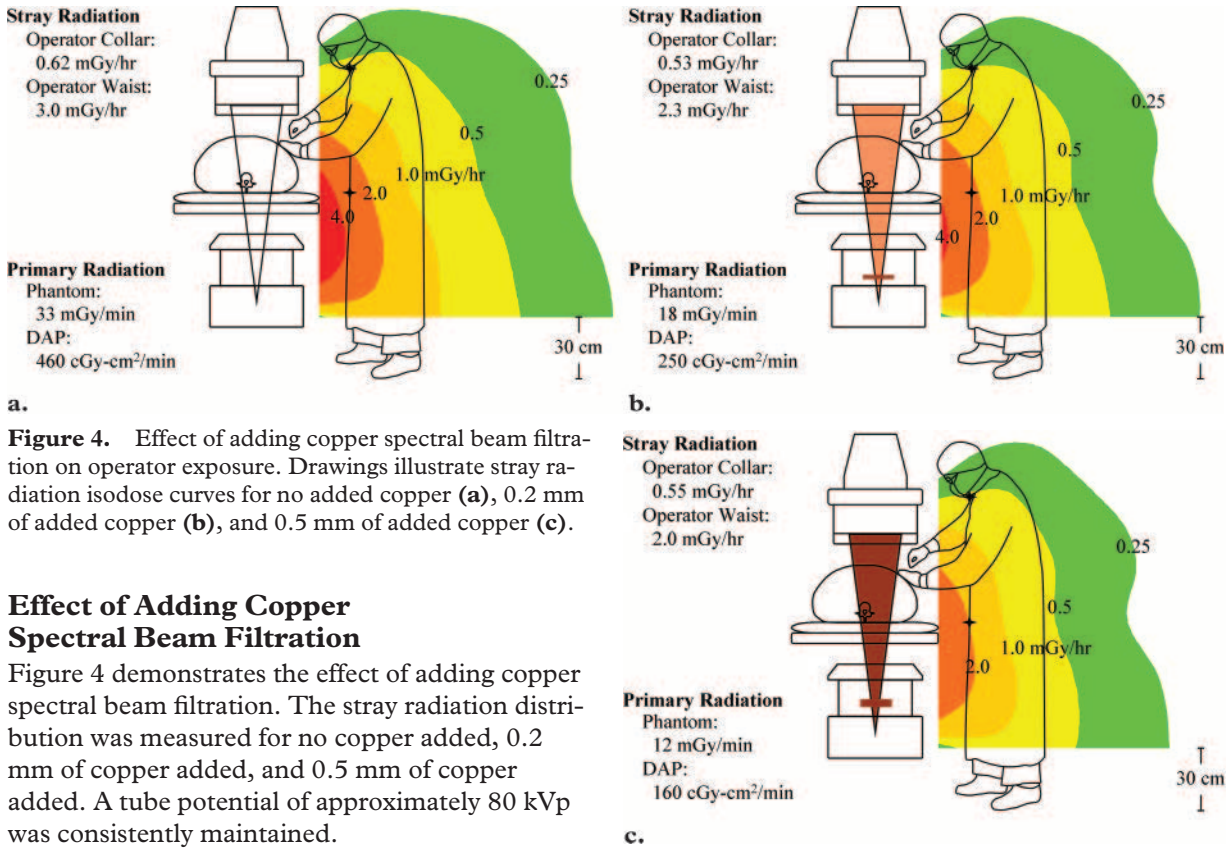

Figure 4. Effect of adding copper spectral beam filtration on operator exposure. Drawings illustrate stray radiation isodose curves for no added copper **(a)**, 0.2 mm of added copper **(b)**, and 0.5 mm of added copper **(c)**.

Effect of Adding Copper Spectral Beam Filtration

Figure 4 demonstrates the effect of adding copper spectral beam filtration. The stray radiation distribution was measured for no copper added, 0.2 mm of copper added, and 0.5 mm of copper added. A tube potential of approximately 80 kVp was consistently maintained.

Teaching Point

Results indicate that both the stray radiation dose rate and the phantom entrance air kerma rate decreased with added filtration. However, dose reduction at the operator's waist was approximately one-half the dose reduction at the phantom entrance. With the addition of 0.2 mm of copper, the phantom entrance air kerma rate and DAP rate dropped by 45%, whereas the stray radiation dose rates at the operator's collar and waist dropped by 13% and 23%, respectively. Similarly, with the addition of 0.5 mm of copper, the phantom entrance air kerma rate and DAP rate dropped by 65%, whereas the stray radiation dose rates at the operator's collar and waist dropped by 11% and 33%, respectively.

Effect of Increasing Patient Abdomen Thickness

The change in stray radiation level that occurs with increasing patient abdomen thickness was simulated under three conditions: phantom alone (24-cm thickness), phantom plus 5 cm of bolus material, and phantom plus 10 cm of bolus material. As Figure 5 demonstrates, there is a significant increase in the stray radiation level as patient size increases. Note that the level increases particularly below the operator's waist. When the phantom thickness is increased from 24 to 29 cm, the phantom entrance air kerma rate increases by a factor of 3.0. Similarly, when the phantom thickness is increased from 29 to 34 cm, the phantom entrance air kerma rate further increases by a factor of 2.6. The increase in operator exposure is somewhat smaller: At the waist, exposure almost doubles with each additional 5 cm of phantom thickness; at the collar, exposure increases by about 30% with each additional 5 cm of phantom thickness.

Teaching Point

Effect of Changing Patient Position

The effect of changing patient position on stray radiation distribution was studied by comparing exposure levels produced with the radiation field centered on the liver versus the spleen. The radiographic technique used for the two positions of the radiation field was nearly the same. As shown in Figure 6, stray radiation levels in the operator's

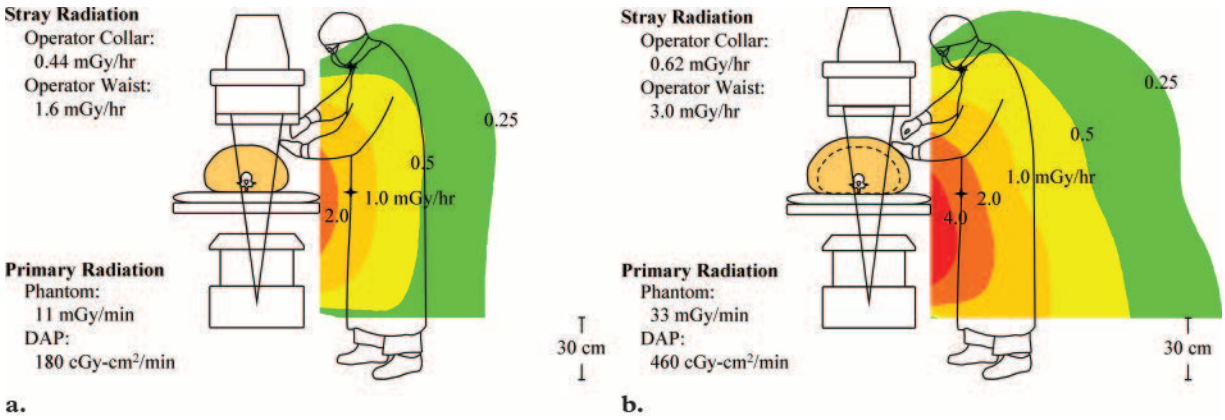

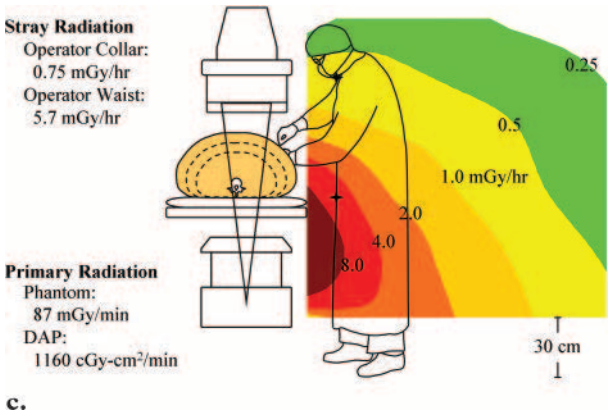

Figure 5. Effect of increasing patient abdomen thickness on operator exposure. Drawings illustrate stray radiation isodose curves calculated with a phantom simulating abdomen thicknesses of 24 cm **(a)**, 29 cm **(b)**, and 34 cm **(c)**.

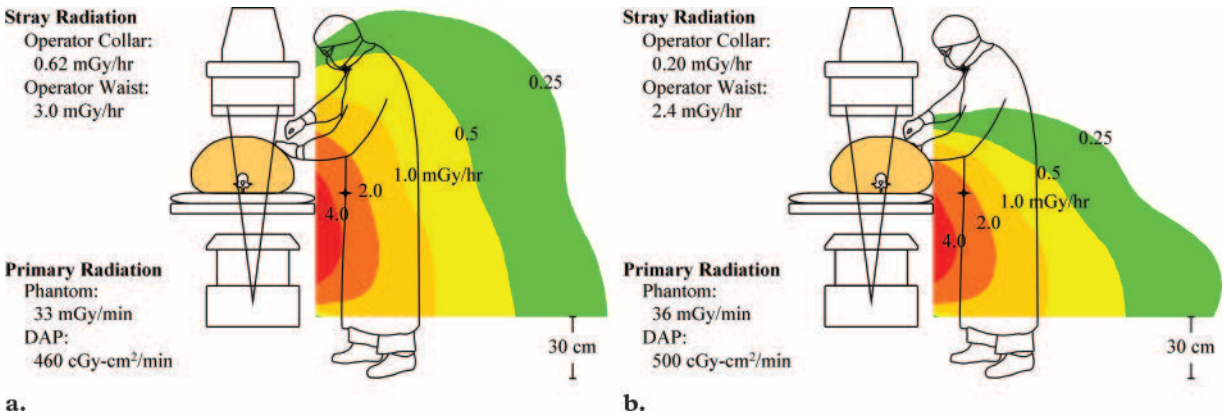

Figure 6. Effect of changing patient position on operator exposure. Drawings illustrate stray radiation isodose curves calculated with the radiation field centered on the liver **(a)** and spleen **(b)**.

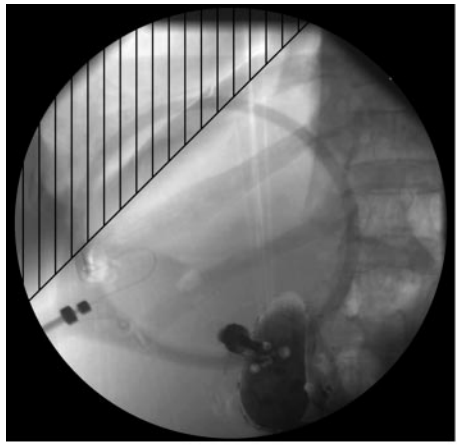

a.

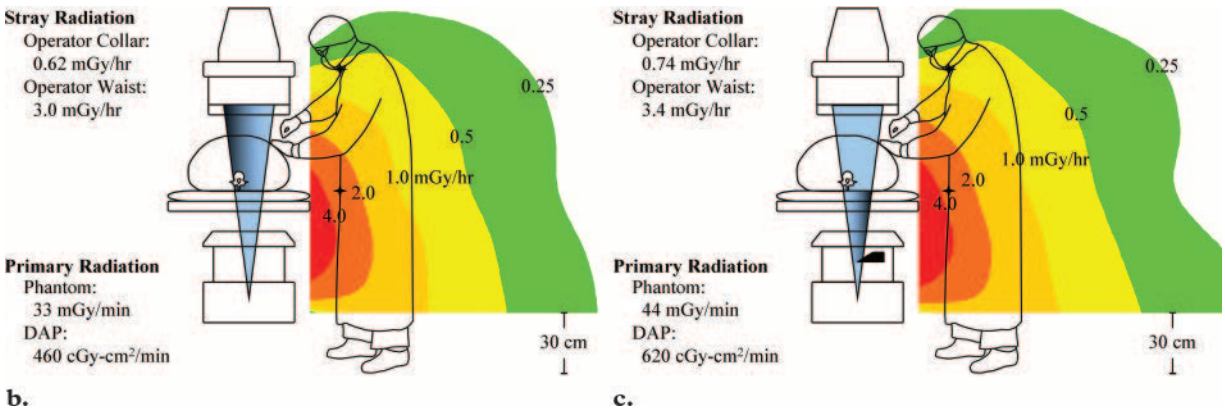

Figure 7. Effect of an equalization filter on operator exposure. **(a)** Fluorographic image shows the position of an equalization filter (shaded area) covering 30% of the FOV. **(b, c)** Drawings illustrate stray radiation isodose curves for configurations without **(b)** and with **(c)** the equalization filter in place.

head and neck region dropped sharply (70% at the collar) when the FOV was shifted to the far side of the phantom. Exposure levels below the operator's waist were relatively unchanged.

Effect of an Equalization Filter

Stray radiation levels were measured both with and without the use of a tapered equalization filter to cover an area of lung within the FOV. The phantom was positioned so that the equalization filter covered approximately 30% of the FOV on the side of the phantom nearer to the operator (Fig 7a). When the wedge filter was inserted, the phantom entrance air kerma rate in the unfiltered area increased by 55%. Averaged over the entire exposed area, the DAP rate increased by 35%. Stray radiation dose rates also increased, but to a lesser degree (ie, by 13% and 19% at the operator's waist and collar, respectively) (Fig 7b, 7c).

Discussion

Several studies have examined the relationship between scatter dose and patient DAP as a basis for assessing occupational exposure (3,9–13). These studies have shown that scatter levels are proportional to DAP for a given distance from the central ray, scattering angle, and x-ray beam energy level. We evaluated the ratio of scatter to DAP, a value known as the scatter factor, under several different imaging conditions. Scatter factors at the operator's waist (45 cm from the central ray, 90° scattering angle) are shown in the Table.

Teaching Point

As mentioned earlier, the highest stray radiation levels occurred with the intermediate-sized FOV (20 cm). This rather puzzling result is made clear when the ratio of scatter to DAP is examined. The scatter factor is the same for each of the three different FOV sizes, indicating that scatter is highest with the highest DAP. For the imaging system used in our study, the 20-cm FOV required the highest DAP rate (610 cGy-cm²/min),

Scatter Factors at the Operator's Waist

Imaging Parameter	Scatter Factor (μGy/Gy-cm²)
FOV (cm)	
28	11
20	11
14	11
Added copper filtration (mm)	
None	11
0.2	15
0.5	21
Patient abdomen thickness (cm)	
24	15
29	11
34	8.2
Patient position	
Exposure field near operator	11
Exposure field far from operator	8.1
Equalization filter	
Without	11
With	9.2

Note.—Distance from central ray = 45 cm, scattering angle = 90°.

even though the highest phantom entrance air kerma rate was seen with the smallest (14-cm) FOV.

As copper spectral beam filtration was added, the scatter factor also increased, nearly doubling with the addition of 0.5 mm of copper. This increase in the scatter factor with increasing hardness of the primary x-ray beam spectrum is consistent with other published findings that the scatter factor increases with increasing tube potential (9–11). One reason for the increase in the scatter factor is that the energy of the scattered x rays increases with the energy of the primary x-ray beam, and these higher-energy scattered x rays are less likely to be attenuated by patient tissue. In addition, the higher-energy scattered x rays produced with the addition of copper filtration are more likely to be transmitted through lead protection devices and garments. As a result, the dose reduction resulting from the use of copper filtration is less than that indicated by the isodose curves for a protected operator (Fig 4).

Note that the scatter factor decreases as patient abdomen thickness increases and as the central ray of the primary beam is moved away from the operator. This decrease is likely due to the increase in attenuating material between the exposed volume and the operator's position. Similarly, the introduction of an equalization filter on the side of the phantom nearer to the operator resulted in an increase in material attenuating the scattered x rays and a concomitant decrease in the scatter factor.

Teaching Point

In addition to the aforementioned variables, several other factors affect operator exposure. Limiting the beam-on time is the most direct dose reduction technique. Fluoroscopic equipment should include a "last image hold" feature to allow image study, discussion, and teaching without added radiation exposure. Beam-on time can also be reduced by implementing a virtual collimation feature, which allows collimator blades to be moved into position prior to imaging. As the isodose curves from this study show, stray radiation levels fall off rapidly with increasing distance from the exposed patient volume. Although the operator generally must remain close to the patient to manipulate interventional devices, various techniques can be used to increase the distance between the operator and the exposed patient volume for at least part of the procedure, including use of a power contrast material injector (14) or vertebroplasty cement injection device (15). Note also the asymmetric distribution of stray radiation (Fig 5c), which results in higher-intensity radiation on the x-ray tube side of the patient. Consequently, it is especially critical in lateral and angulated projections that the operator position him- or herself on the II side of the patient (16) if possible. Use of protective shielding devices can also substantially reduce operator exposure. In addition to lead aprons and other personal protection devices that are worn on the body, shields hung from the ceiling, placed on the floor or table, or placed on the patient have been shown to significantly reduce operator exposure (5,13,17).

As discussed earlier, scatter levels are proportional to patient DAP. Therefore, any technique that reduces patient DAP will also reduce operator exposure. Patient dose reduction methods include low-dose fluoroscopy settings such as

Teaching Point

low-frame-rate pulsed fluoroscopy and grid removal. We have shown that use of copper spectral beam filtration reduces both patient entrance exposure and, to a lesser degree, operator exposure. Use of increased x-ray beam energy would be expected to yield similar results. Incorporation of various image processing features (eg, noise reduction, edge enhancement, contrast enhancement) can allow the use of these low-dose imaging techniques while maintaining adequate image quality. Actions that increase the radiation field size (eg, changing to a larger FOV, moving collimator or equalization filters to the image periphery) will generally decrease patient entrance exposure. However, increasing the field size may either increase or decrease patient DAP, depending on the fluoroscopic system being used. We have shown that some actions that result in an increase in patient entrance exposure (for example, changing to a magnification mode) can result in a decrease in scatter as long as the size of the radiation field decreases enough to result in a decrease in DAP. Reducing the radiation field size may also improve image contrast, provide more uniform image brightness, and reduce glare.

Maintaining operator exposure at a level that is as low as reasonably achievable requires that consideration be given to the equipment and procedure room design features discussed in this article. Furthermore, operators should be aware of the dose reduction techniques described herein and incorporate them into their routine practice as much as possible.

References

1. Marx MV, Niklason L, Mauger EA. Occupational radiation exposure to interventional radiologists: a prospective study. J Vasc Interv Radiol 1992;3:597–606.
2. Niklason LT, Marx MV, Chan H. Interventional radiologists: occupational radiation doses and risks. Radiology 1993;187:729–733.
3. Williams JR. Interdependence of staff and patient doses in interventional radiology. Br J Radiol 1997;70:498–503.
4. Vañó E, González L, Guibelalde E. Radiation exposure to medical staff in interventional and cardiac radiology. Br J Radiol 1998;71:954–960.
5. Whitby M, Martin CJ. Radiation doses to the legs of radiologists performing interventional procedures: are they a cause for concern? Br J Radiol 2003;76:321–327.
6. Balter S. Interventional fluoroscopy. New York, NY: Wiley-Liss, 2001.
7. World Health Organization. Efficacy and radiation safety in interventional radiology. Geneva, Switzerland: World Health Organization, 2000.
8. International Commission on Radiological Protection (ICRP) Publication 85. Avoidance of radiation injuries from medical interventional procedures. Tarrytown, NY: Pergamon, 2000.
9. Boone JM, Levin DC. Radiation exposure to angiographers under different fluoroscopic imaging conditions. Radiology 1991;180:861–865.
10. Marshall NW, Faulkner K. The dependence of the scattered radiation dose to personnel on technique factors in diagnostic radiology. Med Phys 1996;23:1271–1276.
11. Williams JR. Scatter dose estimation based on dose-area product and the specification of radiation barriers. Br J Radiol 1996;69:1032–1037.
12. Servomaa A, Karppinen J. The dose-area product and assessment of the occupational dose in interventional radiology. Radiat Prot Dosimetry 2001;96:235–236.
13. Kuon E, Schmitt M, Dahm JB. Significant reduction of radiation exposure to operator and staff during cardiac interventions by analysis of radiation leakage and improved lead shielding. Am J Cardiol 2002;89:44–49.
14. Hayashi N, Sakai T, Kitagawa M, et al. Radiation exposure to interventional radiologists during manual-injection digital subtraction angiography. Cardiovasc Intervent Radiol 1998;21:240–243.
15. Kallmes DF, O E, Roy SS, et al. Radiation dose to the operator during vertebroplasty: prospective comparison of the use of 1-cc syringes versus an injection device. AJNR Am J Neuroradiol 2003;24:1257–1260.
16. Balter S. Stray radiation in the cardiac catheterization laboratory. In: Nickoloff EL, Strauss KJ, eds. 1998 Syllabus: categorical course in diagnostic radiology physics—cardiac catheterization imaging. Oak Brook, Ill: Radiological Society of North America, 1998; 223–230.
17. Luchs JS, Rosioreanu A, Gregorius D, Venkataramanan N, Keohler V, Ortiz AO. Radiation safety during spine injections. J Vasc Interv Radiol 2005;16:107–111.

An Investigation of Operator Exposure in Interventional Radiology

Beth A. Schueler, PhD et al

RadioGraphics 2006; 26:1533–1541 • **Published online** 10.1148/rg.265055127 • **Content Codes:** PH QA VI

Page 1536
Results indicate that both the stray radiation dose rate and the phantom entrance air kerma rate decreased with added filtration. However, dose reduction at the operator's waist was approximately one-half the dose reduction at the phantom entrance.

Page 1536
There is a significant increase in the stray radiation level as patient size increases.

Page 1538
Scatter levels are proportional to DAP for a given distance from the central ray, scattering angle, and x-ray beam energy level.

Page 1539
The introduction of an equalization filter on the side of the phantom nearer to the operator resulted in an increase in material attenuating the scattered x rays and a concomitant decrease in the scatter factor.

Page 1539
Any technique that reduces patient DAP will also reduce operator exposure.